Photoelectron Spectroscopy and Circular Dichroism in Chiral Biomolecules: L-Alanine

Ivan Powis†

School of Chemistry, University of Nottingham, Nottingham, NG7 2RD, UK

Received: September 16, 1999; In Final Form: December 6, 1999

A theoretical treatment of the photoionization of the chiral amino acid L-alanine is presented. Particular attention is paid to a previously unobserved circular dichroism which should be detectable in the photoelectron angular distribution (CDAD) from randomly oriented molecules. Numerical estimates of this difference in the differential cross-sections for left- and right-circularly polarized light range as large as 40% of the mean cross-section. Three different low-energy conformational structures are considered. Further comparisons with the experimental photoelectron spectrum suggest, however, that only one dominates in the gas phase. This concurs with other experimental data but disagrees with conclusions drawn from previous molecular orbital calculations. The magnitude of the predicted CDAD effect, especially when ionizing skeletal bonding orbitals, is sufficient to suggest that it may provide an experimental means for successfully distinguishing optical and conformational isomers.

Although circular dichroism in the absorption spectra of optical isomers is a well-known effect, it is comparatively weak (the difference between response to left- and right-circularly polarized light being usually less than 10^{-4} of the total). However, another, more pronounced form of dichroism can occur in measurements of the *differential* photoionization cross-section.[1] Whereas absorption dichroism results from quantum interference between electric- and the much weaker magnetic-dipole terms in the total cross-section (and is consequently difficult to interpret and model a priori), circular dichroism in the photoelectron angular distribution (CDAD) arises from the stronger interference between pure electric dipole terms in the differential cross-section.[1,2]

Until the present time theoretical and practical investigation of molecular CDAD has focused on the behavior of the spatially oriented or aligned diatomic species CO[3−7] and NO.[5,7−9] Target molecule alignment allows a requisite "handedness" to be created in the experimental geometry (molecular axis plus photon and photoelectron directions), and can be accomplished experimentally by surface adsorption,[5,7,10] photoalignment in REMPI processes,[8,9] or the investigation of electron−ion recoil vector correlations in dissociative ionization.[6] These results for oriented diatomic molecules (and also for the polyatomics CH_3I and benzene[7]) confirm expectations of a CDAD signal comparable in magnitude to the differential cross-section.

However, the original predictions[1,2] also made clear that the CDAD effect should be observable in chiral molecules, even when these are *randomly* oriented. In fact the lab-frame photoelectron angular distribution for circularly polarized ionizing radiation can be shown to take the form:[2,11]

$$I_p(\theta) = 1 + b_1^p P_1(\cos\theta) + b_2^p P_2(\cos\theta) \qquad (1)$$

where the index $p = +1$ (-1) signifies left (right) circularly polarized light. The coefficients of the second Legendre polynomial term are $b_2^{+1} = b_2^{-1} \equiv -1/2\ \beta$, where β is the traditional photoelectron asymmetry parameter obtained with linearly polarized light; the first Legendre polynomial coefficients, $b_1^{\pm 1}$, are zero for all but chiral molecules in which particular case they are related by $b_1^{+1} = -b_1^{-1}$. (It may also be

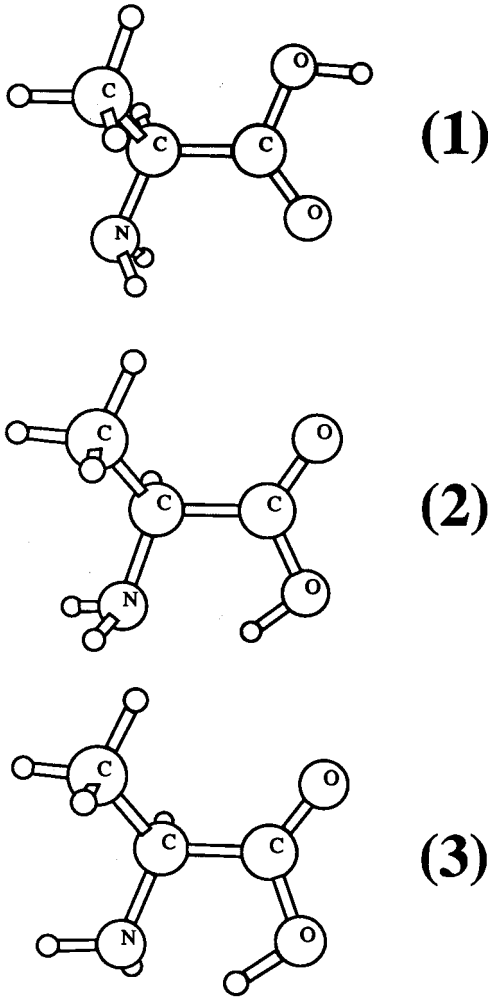

Figure 1. Low-energy conformers of L-alanine.

† Telephone: 44 115 951 3467. Fax: +44 115 951 3562. E-mail: ivan.powis@nottingham.ac.uk.

10.1021/jp9933119 CCC: $19.00
Published on Web 01/13/2000

TABLE 1: Energies of L-Alanine Conformers

	B3LYP/6-31G**[a]		6-311++G** MP2[b]	
conformer	absolute (au)	relative (cm^{-1})	absolute (au)	relative (cm^{-1})
1	−323.757173		−323.103013	
2	−323.757710	−118	−323.102783	51
3	−323.756963	+46	−323.102256	166

[a] This work. [b] Ref 22.

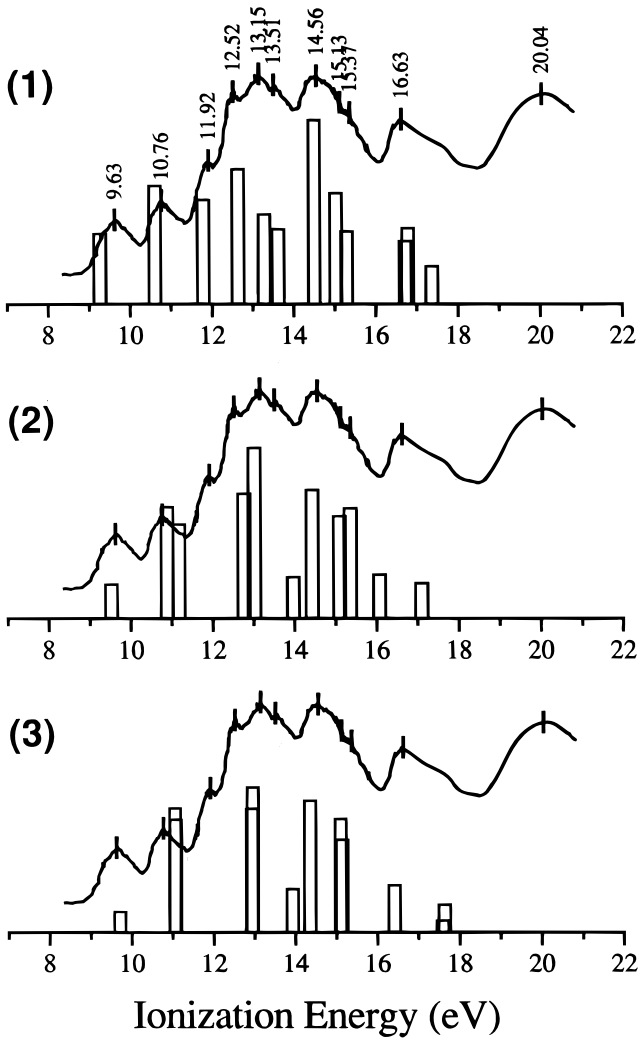

Figure 2. Photoelectron spectrum of alanine[29] compared with calculated ROVGF/cc-pVDZ ionization energies for conformers (**1**)−(**3**). The height of each calculated bar is proportional to its CMS-Xα cross-section. Peak location software was used to identify marked peak positions in the experimental spectrum.

noted that the b_1^p coefficients for a D- and L- enantiomer pair are simply related by a sign change.) From eq 1 and the preceding relationships the CDAD signal may be written:

$$I_{+1}(\theta) - I_{-1}(\theta) = (b_1^{+1} - b_1^{-1})\mathrm{P}_1(\cos\theta) = 2b_1^{+1}\cos\theta \quad (2)$$

Numerical CDAD estimates for randomly oriented chiral molecules may thus be obtained by calculating electric dipole photoionization matrix elements and hence the b_j^p coefficients, as recently done for the first time for D-glyceraldehyde and D-lactic acid.[11] In this communication photoionization of the gaseous amino acid L-alanine (CH_3CHNH_2COOH) is investigated. Current ab initio approaches to the calculation of the required non-$\mathbf{L}^2$ continuum functions are not feasible for such

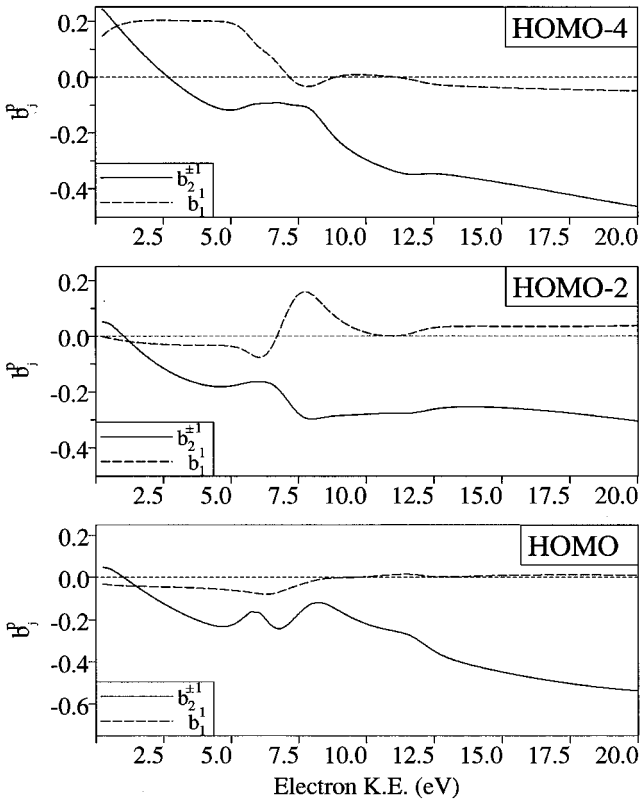

Figure 3. CMS-Xα photoelectron anisotropy parameters for circularly polarized photoionization of the indicated orbitals of L-alanine (**1**) leading to the ground, second, and fourth excited electronic states of the ion.

large molecules which lack simplifying symmetry elements and the CMS-Xα continuum multiple scattering treatment, utilizing an Xα local-exchange potential, has been used for this purpose.[12,13] This method is well established for calculating total cross-sections and β parameters of, for example, rigid polyatomic molecules[14−19] and has recently been shown to be capable of providing a good account of doubly differential molecule-frame cross-sections in CF_3I,[20,21] a far more stringent test of the method.

The CMS-Xα calculations assume a fixed molecular geometry. Unlike almost all previous applications, however, gaseous alanine cannot be simply considered as a rigid molecule. Recent calculations identify a number of low-lying conformations,[22,23] such that several may be expected to coexist in a sample at thermal equilibrium. But rotational spectra recorded in a free-expansion jet identify only a single dominant conformer [(**1**)—see Figure 1] with (**2**), the only other structure detected, being one-eighth less populated.[24] Similarly, gas-phase electron diffraction results[25] were explained by reference to just the single conformation (**1**).

The three lowest-lying conformers identified by earlier calculations[22−24] (**1**−**3** in Figure 1) have been considered in this work. To obtain a complete set of geometric parameters for each conformation, full density functional geometry optimization calculations were performed using a B3LYP functional[26,27] and 6-31G** basis set, as implemented in the Gaussian 94 package.[28] As expected these structures are predicted to lie within a few hundred cm^{-1} of each other (Table 1). Model Xα potentials were then obtained for each B3LYP/6-31G** molecular geometry and subsequently used to calculate the ground state−continuum matrix elements for each assumed conformation. Further details of the method and procedures adopted may be found in ref 11.

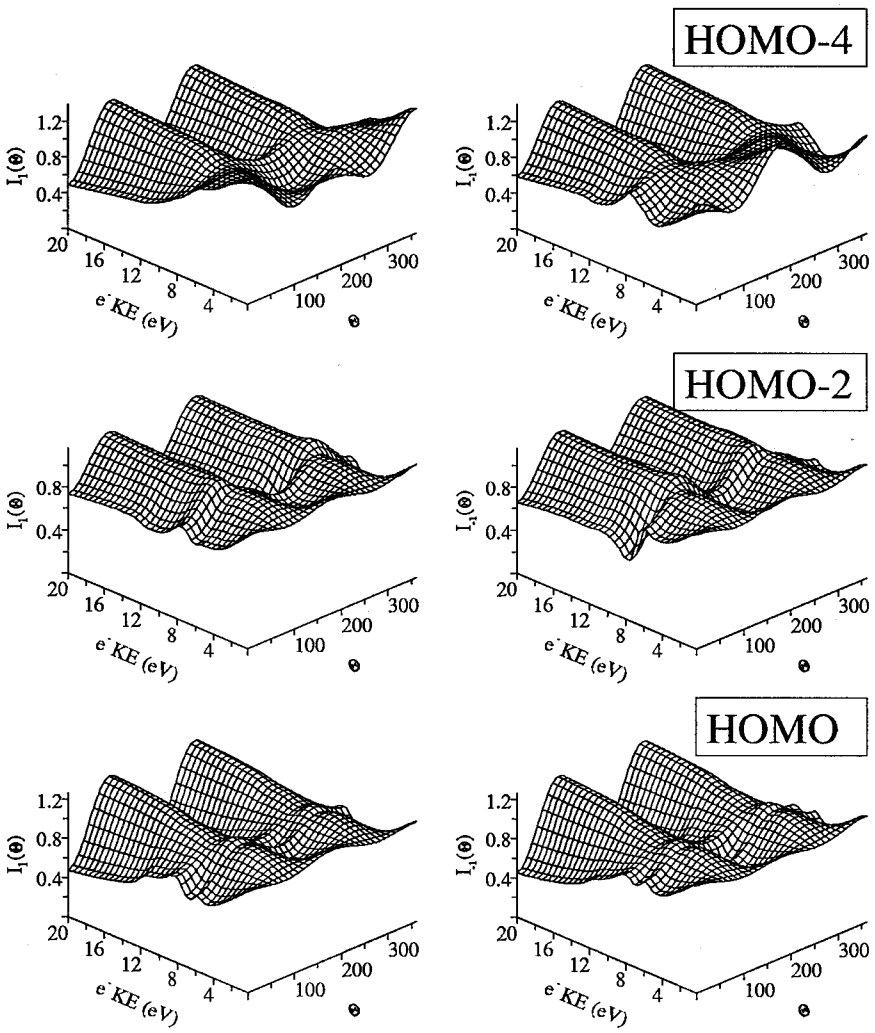

Figure 4. Photoelectron angular distributions, $I_{\pm1}(\theta)$, as a function of electron energy for photoionization of the indicated orbitals of L-alanine (**1**).

The gas-phase photoelectron spectrum (PES) of L-alanine[29] shows a number of well-resolved bands. Theoretical estimates of the vertical ionization energies for each optimized B3LYP/6-31G** geometry (**1**−**3**) were calculated using an outer-valence Green's function (OVGF) method[30,31] and a cc-pVDZ basis, again as implemented in the Gaussian 94 package.[28] These calculated values and the experimental PES are compared in Figure 2. It can be seen that there is an exceptionally good correlation between experimental and calculated peak positions for (**1**). In contrast, the calculated ionization energies for (**2**) and (**3**) are much less well correlated with experiment and would appear to make no significant contribution to enhancing the overall agreement between experiment and theory, except perhaps for the lowest energy PES band. The PES data in Figure 2 therefore leads one to concur with the proffered interpretations of millimeter-wave[24] and electron diffraction[25] studies, that structure (**1**) is in fact the dominant experimental gas-phase conformation.

CMS-Xα results for the electron angular distribution parameters following photoionization by left circularly polarized light are shown for three representative orbitals of conformer (**1**) in Figure 3. Some of the structure evident in the curves can be associated with a broad predicted shape resonance in the electron continuum, at kinetic energies in the range 5−8 eV, and a second weaker resonance at ∼12 eV. These resonances influence, to some degree, the ionization of all other valence orbitals of all three studied conformers. A caveat is, however, appropriate in that a well-established limitation of the CMS-Xα method is its propensity to overestimate the magnitude and sharpness of shape resonance features.

For ionization of the HOMO (outermost valence orbital), the chiral anisotropy parameter is small, $|b_1^1| \leqslant .05$, and is significantly less than typical values previously obtained for glyceraldehyde and lactic acid.[11] Similarly, for the next two molecular orbitals in sequence, the HOMO-1 and HOMO-2, although in the latter case b_1^1 is enhanced around the lower energy shape resonance (Figure 3). However, these outer orbitals are highly localized on the N (HOMO) and O atoms (HOMO-1,-2), an assignment[29] confirmed by the present calculations. It is then possible to rationalize the small b_1^1 parameters seen here by arguing that what are essentially lone-pair electrons, localized away from the asymmetric carbon center, are unlikely to be greatly sensitive to the chirality of the molecular scattering potential. Conversely, the increase in b_1^1 displayed by the HOMO-2 orbital at ∼7.5 eV suggests that the increased electron−ion core coupling at shape resonance may allow the electron to become more sensitive to the molecular potential.

The third example chosen to be presented in Figure 3 is the ionization of the HOMO-4 orbital of (**1**), which is the first skeletal σ-bonding orbital. Now the calculated b_1^1 parameter is significantly bigger than in the previous examples, and indeed its magnitude is comparable to, or even greater than, the b_2^1 (β) parameter. This helps corroborate an inference from the preceding rationalization, that delocalized initial orbitals should display greater sensitivity to the asymmetric chiral molecular framework.

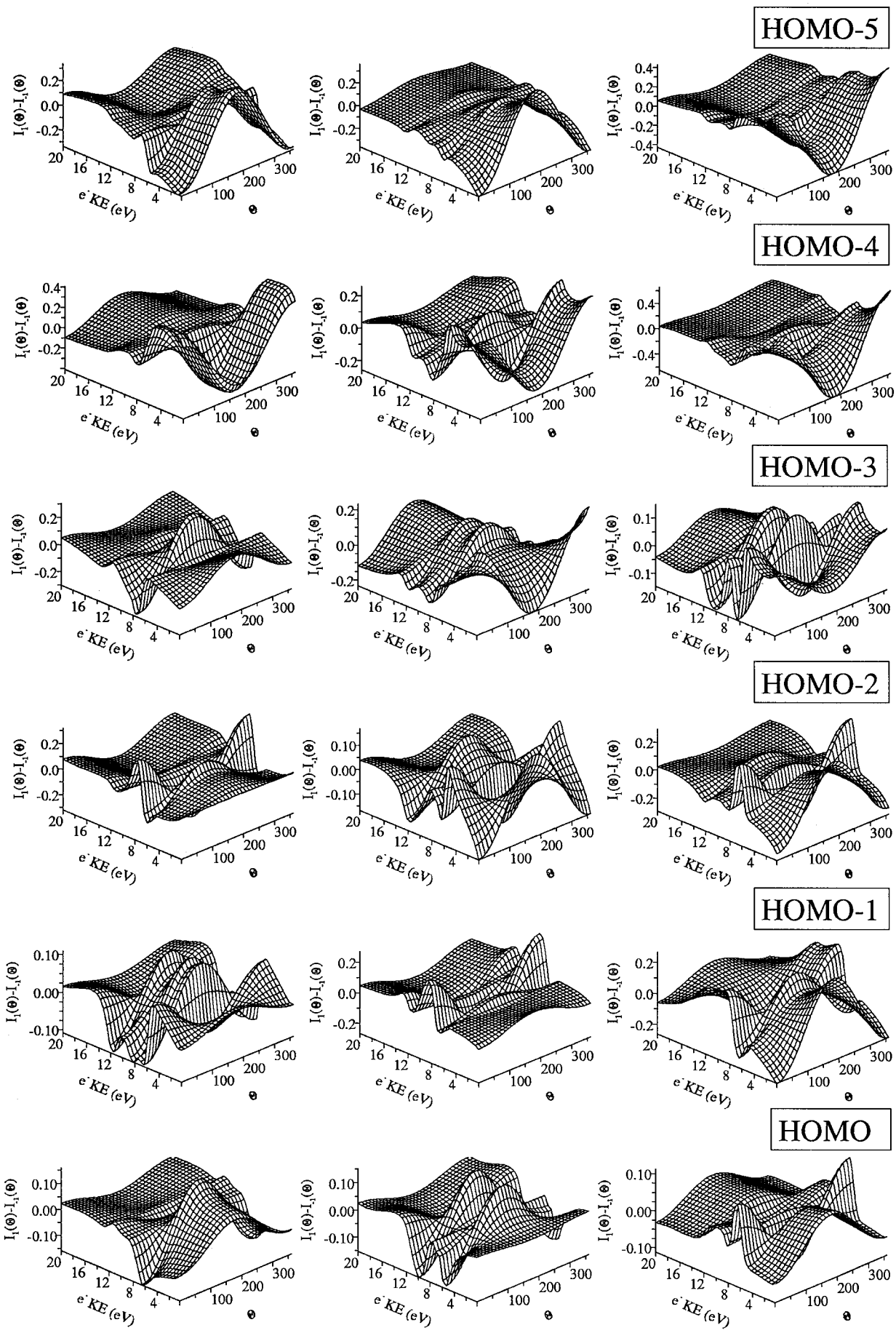

Figure 5. Predicted circular dichroism (CDAD) for ionization of the six outermost orbitals of L-alanine: bottom row, HOMO; top row, HOMO-5; Left column, conformer (**1**); middle column, conformer (**2**); right column, conformer (**3**).

Even so, in this and all other calculations that have been performed but not explicitly reported here, the magnitude of the b_1^1 parameter tends to zero as the electron kinetic energy extends above a few tens of eV. A similar observation was made for glyceraldehyde and lactic acid[11] and, as there, it can be supposed that the faster escaping electrons become less sensitive to scattering by the molecular ion core.

The b_j^p anisotropy parameters may be used to evaluate the electron angular distributions $I_p(\theta)$ (eq 1) and for each of the preceding three examples these are drawn in Figure 4 as a function of electron kinetic energy for both left and right circularly polarized light. Common to all is (a) the behavior at ~20 eV as the $b_2^{\pm 1}$ anisotropy parameter (the β parameter for circularly polarized light) comes to dominate the angular distribution which thus peaks at 90° and 270° to the photon propagation direction—i.e., the classical result with electrons ejected in the plane containing the radiation electric vector; (b) a "crease" at ~8 eV resulting from the shape resonance in that region. However, at least for HOMO-4 the $I_{\pm 1}(\theta)$ curves are distinctly different at lower electron energies, which is the different chiral response envisaged in the preceding discussion.

Finally, the calculated CDAD signals for ionization of the six outermost orbitals of each of (**1**), (**2**), and (**3**) are plotted in Figure 5. Unsurprisingly now, CDAD is greatest for the skeletal σ-bonding orbitals, HOMO-5 and HOMO-4, at energies from threshold to ~8 eV, with a difference between the forward and backward scattering directions approaching ±0.4 (i.e., nearly ±40% of the mean) for (**1**) and (**3**). This is similar to previous findings for glyceraldehyde and lactic acid,[11] and suggests that CDAD in such cases should be readily detectable by experiments. Even in the other cases shown here the maximum CDAD response is at least ±0.1 and often ±0.2 or more. Sometimes this is found near threshold, sometimes around the shape resonance energies. While repeating the caveat about CMS-Xα overestimating resonance effects, this suggests that a measurable CDAD might be obtained in most cases with there being a possibility of distinguishing enantiomers by the sign of an observed CDAD signal. More speculatively, the clear differences between the CDAD responses predicted for different conformers (see Figure 5) may permit structural insight to be gleaned from experimental measurements of this phenomenon.

References and Notes

(1) Cherepkov, N. A. *Chem. Phys. Lett.* **1982**, *87* (4), 344−348.
(2) Ritchie, B. *Phys. Rev. A* **1976**, *13*, 1411−1415.
(3) Dubs, R. L.; Dixit, S. N.; McKoy, V. *Phys. Rev. Lett.* **1985**, *54* (12), 1249−1251.
(4) Westphal, C.; Bansmann, J.; Getzlaff, M.; Schönhense, G. *Phys. Rev. Lett.* **1989**, *63*, 151−154.
(5) Westphal, C.; Fegel, F.; Bansmann, J.; Getzlaff, M.; Schönhense, G.; Stephens, J. A.; McKoy, V. *Phys. Rev. B* **1994**, *50* (23), 17534−17539.
(6) Heiser, F.; Gessner, O.; Hergenhahn, U.; Viefhaus, J.; Wieliczek, K.; Saito, N.; Becker, U. *J. Elec. Spec. Relat. Phenom.* **1996**, *79*, 415−417.
(7) Westphal, C.; Bansmann, J.; Getzlaff, M.; Schönhense, G.; Cherepkov, N. A.; Braunstein, M.; McKoy, V.; Dubs, R. L. *Surf. Sci.* **1991**, *253* (1−3), 205−219.
(8) Appling, J. R.; White, M. G.; Dubs, R. L.; Dixit, S. N.; McKoy, V. *J. Chem. Phys.* **1987**, *87* (12), 6927−6933.
(9) Leahy, D. J.; Reid, K. L.; Park, H. K.; Zare, R. N. *J. Chem. Phys.* **1992**, *97* (7), 4948−4957.
(10) Westphal, C.; Bansmann, J.; Getzlaff, M.; Schönhense, G. *Vacuum* **1990**, *41* (1−3), 87−89.
(11) Powis, I. *J. Chem. Phys.* **2000**, *112*, 301−310.
(12) Dill, D.; Dehmer, J. L. *J. Chem. Phys.* **1974**, *61*, 692−699.
(13) Davenport, J. W. *Phys. Rev. Lett.* **1976**, *36*, 945−948.
(14) Stephens, J. A.; Dill, D.; Dehmer, J. L. *J. Chem. Phys.* **1986**, *84* (7), 3638−3646.
(15) Swanson, J. R.; Dill, D.; Dehmer, J. L. *J. Chem. Phys.* **1981**, *75*, 619−624.
(16) Addison, B. M.; Tan, K. H.; Bancroft, G. M.; Cerrina, F. *Chem. Phys. Lett.* **1986**, *129* (5), 468−474.
(17) Yates, B. W.; Tan, K. H.; Bancroft, G. M.; Coatsworth, L. L.; Tse, J. S. *J. Chem. Phys.* **1985**, *83* (10), 4906−4916.
(18) Tse, J. S.; Liu, Z. F.; Bozek, J. D.; Bancroft, G. M. *Phys. Rev. A* **1989**, *39* (4), 1791−1799.
(19) Powis, I. *Chem. Phys.* **1995**, *201* (1), 189−201.
(20) Downie, P.; Powis, I. *Phys. Rev. Lett.* **1999**, *82*, 2864−2867.
(21) Downie, P.; Powis, I. *J. Chem. Phys.* **1999**, *111*, 4535−4547.
(22) Csaszar, A. G. *J. Phys. Chem.* **1996**, *100*, 0(9), 3541−3551.
(23) Kaschner, R.; Hohl, D. *J. Phys. Chem. A* **1998**, *102* (26), 5111−5116.
(24) Godfrey, P. D.; Firth, S.; Hatherley, L. D.; Brown, R. D.; Pierlot, A. P. *J. Am. Chem. Soc.* **1993**, *115*, 5 (21), 9687−9691.
(25) Iijima, K.; Beagley, B. *J. Mol. Struct.* **1991**, *248* (1−2), 133−142.
(26) Becke, A. D. *J. Chem. Phys.* **1993**, *98* (7), 5648−5652.
(27) Lee, C. T.; Yang, W. T.; Parr, R. G. *Phys. Rev. B* **1988**, *37* (2), 785−789.
(28) Frisch, M. J.; Trucks, G. W.; Schlegel, H. B.; Gill, P. M. W.; Johnson, B. G.; Robb, M. A.; Cheeseman, J. R.; Keith, T.; Petersson, G. A.; Montgomery, J. A.; Raghavachari, K.; Al-Laham, M. A.; Zakrzewski, V. G.; Ortiz, J. V.; Foresman, J. B.; Cioslowski, J.; Stefanov, B. B.; Nanayakkara, A.; Challacombe, M.; Peng, C. Y.; Ayala, P. Y.; Chen, W.; Wong, M. W. A.; J. L.; Replogle, E. S.; Gomperts, R.; Martin, R. L.; Fox, D. J.; Binkley, J. S.; Defrees, D. J.; Baker, J.; Stewart, J. P.; Head-Gordon, M.; Gonzalez, C.; Pople, J. A. *Gaussian 94*, Revision E.3; *Gaussian 94*, Revision E.3; Gaussian Inc., Pittsburgh, PA.
(29) Klasinc, L. *J. Elec. Spec. Relat. Phenom.* **1976**, *8*, 161−164.
(30) von Niessen, W.; Schirmer, J.; Cederbaum, L. S. *Comput. Phys. Rep.* **1984**, *1* (2), 57−125.
(31) Zakrzewski, V. G.; Dolgounitcheva, O.; Ortiz, J. V. *J. Chem. Phys.* **1996**, *105* (19), 8748−8753.